8-2016

Sparse representation for the ISAR image reconstruction

Mengqi Hu
The University of Texas Rio Grande Valley

SPARSE REPRESENTATION FOR THE ISAR IMAGE RECONSTRUCTION

A Thesis

by

MENGQI HU

Submitted to the Graduate College of
The University of Texas Rio Grande Valley
In partial fulfillment of the requirements for the degree of

MASTER OF SCIENCE

August 2016

Major Subject: Mathematics

SPARSE REPRESENTATION FOR THE ISAR IMAGE RECONSTRUCTION

A Thesis
by
MENGQI HU

COMMITTEE MEMBERS

Dr. Zhijun Qiao
Chair of Committee

Dr. Bin Fu
Committee Member

Dr. Jasang Yoon
Committee Member

Dr. Ranadhir Roy
Committee Member

August 2016

ABSTRACT

Hu, Mengqi, Sparse Representation For The ISAR Image Reconstruction . Master of Science (MS), August, 2016, 29 pp, 1 table, 12 figures, 23 references, 26 titles.

In this thesis, a sparse representation for the data form a multi-input multi-output based inverse synthetic aperture radar (ISAR) system is derived for two dimensions. The proposed sparse representation motivates the use a of a Convex Optimization directly that recovers the image without the loss information of the image with far less samples that that is required by Nyquist−Shannon sampling theorem, which increases the efficiency and decrease the cost of calculation in radar imaging.

DEDICATION

This is dedicated to my family and friends for their love, support, and confidence in me.

ACKNOWLEDGMENTS

This work would have not been possible without the help of my advisor and mentor Dr. Zhijun Qiao and his imaging group for their support during my academic career. I would also like to thank the many teachers in my life for their patience and ability to show the beauty of mathematics.

TABLE OF CONTENTS

LIST OF FIGURES

Page

CHAPTER I

INTRODUCTION

MIMO radar is a very recent developed technology that is attracting the attention of researchers. Unlike a traditional phased-array radar,which uses same waveform with different scaled version and phase as its transmitted signal, a MIMO radar system transmits signal with different waveform and phases. This diversity in waveform provides a MIMO radar system a great advantage comparing against a normal radar system [12, 13, 25].

Inverse synthetic Aperture radar(ISAR) has been in development for more than 50 years. It is a very important sensing technique providing the opportunity to collect data over a moving object with the potential for high resolution [7, 9]. An ISAR system is based on relatively stationary platforms such as a radar system settled on an island, mountain or so.

An ISAR system based on MIMO technique has some significant advantages comparing with the tradition radar systems. For example, the cross-range resolution of an ISAR system is ρ_c, and we have $\rho_c = \lambda/2\Delta\theta = \lambda\ 2\omega T$, where λ is the wavelength, $\Delta\theta$ is the variation of the aspect angle during the coherent processing interval (CPI), ω is the rotational angular velocity, and T is the CPI[7]. There are two main methods to improve the resolution here. One is to reduce the wavelength λ which is restricted by the hardware. The other one is to shorten T which MIMO helps a lot by y partially using space sampling instead of the time sampling [26]. Theoretically, we can directly use a real aperture antenna array to achieve multiple radar detection and imaging, but doing it this way will need too many antennas such that our current capability of hardware cannot support such a system. Luckily, the MIMO technique allows us to use an equivalent receiving array in stead of a real receiving array and hence we could still obtain a high resolution image using a smaller real

antenna array.[1, 2]

Nowadays as the technology improves, the growing needs for high resolution of an ISAR image lead to a significant increase of the data size that is collected from the target. It costs a lot of time and space to restore and process these data and form the data into an image. This motivates the scientific research in Compressive Sensing (CS). Compressive sensing – also known as compressed sensing, compressive sampling, or sparse sampling – is a signal processing technique for efficiently acquiring and reconstructing a signal. This is based on the principle that, through optimization, the sparsity of a signal can be exploited to recover it from far fewer samples than required by the Shannon-Nyquist sampling theorem.[4, 6, 5]

1.1 Thesis Chapter Outline

The rest of this thesis is organized as followed:

Chapter 2:

In this chapter we provide inverse synthetic aperture radar, MIMO system and compressive sensing formulations

Chapter 3:

In this chapter we will we will present the proposed reconstruct algorithm and show some simulation results

Chapter 4:

Conclusion and future work.

CHAPTER II

MIMO ISAR MODELING

2.1 ISAR Modeling

We start with the model of an ISAR system which is what our proposed algorithm is based on. Radar waves are electromagnetic waves and hence are governed by Maxwell's equations.Rather than using the full Maxwell equations, we use a simplified scalar model[7]

$$\left(\nabla^2 - \frac{1}{c(x)}\frac{\partial^2}{\partial t^2}\right)\mathscr{E}(t,x) = 0 \tag{2.1}$$

in which $c(\mathbf{x})$ is the propagation speed of electromagnetic wave and $\mathscr{E}(t,x)$ stands for the electric field which spread in the free space following wave equation. See that in free space $c(\mathbf{x}) = c_0$. This equation is a good model for the propagation of each Cartesian component of the electric field. Scattering can be considered as a result of perturbations in the wave speed, which can be written as

$$\frac{1}{c^2(\mathbf{x})} = \frac{1}{c_0^2} - V(x) \tag{2.2}$$

where $V(\mathbf{x}$ stands for the reflectivity function. Equations (2.1), (2.2) are very commonly used model for radar scattering, but we need to notice that $V(x)$ dose not correspond to the perturbation in the electromagnetic wave speed exactly. It is actually a measure of the radar polarized reflectivity measured by the antenna. More accurate models can be found in [3] and references there. For a moving target, we use $V(x,t)$ instead of the original stationary reflectivity function.

The fundamental solution[22] to the wave equation will help us modeling the scattering and it is a generalized function satisfying

$$(\nabla^2 - c_0^{-2}\partial_t^2)g(t,x) = -\delta(t)\delta(x) \tag{2.3}$$

The solution to equation (2.3) is

$$g(t,\mathbf{x}) = \frac{\delta(t-|\mathbf{x}|/c_0)}{4\pi|\mathbf{x}|} = \int \frac{e^{-i\omega(t-|x|/c_0)}}{8\pi^2|\mathbf{x}|} d\omega \tag{2.4}$$

Here $g(t,\mathbf{x})$ is the field at $(t,\mathbf{x})$ generated by the source. If the source is located at the origin and starts at time 0, it is called the outgoing fundamental solution or Green's function[19].

With the help of Green's function we can solve the wave equation under the constant-speed condition with any source term. Particularly, we have the following result.

$$(\nabla^2 - c_0^{-2}\partial_t^2)u(t,x) = -j(t,\mathbf{x}) \tag{2.5}$$

$$u(t,\mathbf{x}) = -\int g(t-t',x-y)\, j(t',y)\, dt'dy \tag{2.6}$$

The solution of equation (2.5) is (2.6) where j stands for the source of the wave. In frequency domain, the above result can be written as

$$(\nabla^2 + k^2)G = -\delta \tag{2.7}$$

$$G(\omega,x) = \frac{e^{ik|x|}}{4\pi|x|} \tag{2.8}$$

Now we apply the wave equation to the electronic field. We know that $\mathscr{E}^{tot} = \mathscr{E}^{in} + \mathscr{E}^{sc}$, where $\mathscr{E}^{tot}, \mathscr{E}^{in}, \mathscr{E}^{sc}$ are total field, incidental field and scattered field respectively and for simplification we assume that we have free space.Therefore, we have

$$(\nabla^2 - c^{-2}(x)\partial_t^2)\mathscr{E}^{tot}(t,x) = j(t,x) \tag{2.9}$$

$$(\nabla^2 - c_0^{-2}\partial_t^2)\mathscr{E}^{in}(t,x) = j(t,x) \tag{2.10}$$

where j stand for the source of the field or equivalently, the current density on the transmitting antenna. Substituting equation (2.1) to (2.9) and then subtract (2.10), we have the equation for scattered field

$$(\nabla^2 - c_0^{-2}\partial_t^2)\mathscr{E}^{sc}(t,x) = -V(x)\partial_t^2\mathscr{E}^{tot}(t,x) \tag{2.11}$$

Considering $j = V(x)\partial_t^2\mathscr{E}^{tot}$, the equation (2.11) has the same form of (2.5). We can use the result of (2.6) to solve it which is

$$\mathscr{E}^{sc} = \iint g(t-\tau,x-z)V(z)\partial_t^2\mathscr{E}^{tot}\, d\tau dz \tag{2.12}$$

Apply (2.4) to (2.12) we have

$$\mathscr{E}^{sc} = \iint \frac{\delta(t-\tau-|x-z|/c)}{4\pi|x-z|} V(z)\partial_t^2 \mathscr{E}^{tot} d\tau dz \tag{2.13}$$

See that $\mathscr{E}^{tot} = \mathscr{E}^{in} + \mathscr{E}^{sc}$, $\mathscr{E}^{sc}$ appears on both sides of (2.13). This means (2.13) is not a formula but an equation to be solved for $\mathscr{E}^{sc}$. For solving this problem we Fourier transform the problem into frequency domain.

$$E(\omega) = \int e^{i\omega t} \mathscr{E} dt \tag{2.14}$$

Thus by (2.7) and (2.8) we have

$$(\nabla^2 + \frac{\omega^2}{c^2(x)}) E^{tot} = J(\omega, x) \tag{2.15}$$

$$(\nabla^2 + \frac{\omega^2}{c_0^2}) E^{in} = J(\omega, x) \tag{2.16}$$

and hence (2.13) becomes

$$E^{sc}(\omega, \mathbf{x}) = -\int \frac{e^{ik|x-z|}}{4\pi|x-z|} V(\mathbf{z})\omega^2 E^{tot}(\omega, \mathbf{z}) d\mathbf{z} \tag{2.17}$$

Note that (2.17) can be written as

$$E^{sc} = -\mathscr{G}\mathscr{V} E^{tot} \tag{2.18}$$

where $\mathscr{G}$ denotes the operator of convolution with Green's function and $\mathscr{V}$ denotes the operator of multiplication by $V\omega^2$. Thus we have

$$E^{tot} = E^{in} - \mathscr{G}\mathscr{V} E^{tot} \tag{2.19}$$

We could solve the problem (2.19) by $E^{in} = (\mathscr{I} + \mathscr{G}\mathscr{V}) E^{tot}$ using Neumann series

$$E^{tot} = (\mathscr{I} + \mathscr{G}\mathscr{V})^{-1} E^{in} = \sum_{n=1}^{\infty} (-1)^n (\mathscr{I} + \mathscr{G}\mathscr{V})^n E^{in} \tag{2.20}$$

The series converges when the operator $\mathscr{G}\mathscr{V}$ is small in some sense[18] which leads to a weak-scattering assumption.

Explicitly, equation (2.19) can be written as

$$\begin{aligned} E^{tot}(x) =& E^{in} + \int G(x-x')V(x')\omega^2 E^{in}(x')dx' \\ &+ \int G(x-x')V(x')\omega^2 \int G(x'-x'')V(x'')\omega^2 E^{in}(x'')dx'dx'' + \cdots \end{aligned} \tag{2.21}$$

In the (2.21), the first term on the right side stands for the incident field, second term stands for the field that is scattered by scatterer at $\mathbf{x}'$ with strength $V(\mathbf{x}')\omega^2$ and then propagated to the measurement location at x, the third term is the field scattered at X'' first with strength $V(\mathbf{x}')\omega^2$ and then propagated to X', scattered again at $\mathbf{x}'$ with strength $V(\mathbf{x}')\omega^2$ and then propagated to the measurement location at x. For imaging purpose, we measure $E^s c$ at the antenna, and we would like to determine the reflectivity function V. However they are both unknown in the neighborhood of target V. Therefore, we need to apply Born approximation, also known as weak-scattering or single-scattering approximation. The Born approximation drops all terms in (2.21) that has more than 1 factor of V and hence we have

$$E^{sc} \approx E_B^{sc} := -\int \frac{e^{ik|x-z|}}{4\pi|x-z|} V(\mathbf{z})\omega^2 E^{in}(\omega,\mathbf{z})d\mathbf{z} \tag{2.22}$$

Here E^{in} can be obtained by solving (2.10). Since in most cases, the distance between the target and antenna is far larger than the size of an antenna, here we use a point like antenna for simplification. So we have $j(t,x) = p(t)\delta(x-x^0)$ where p is the waveform of transmitted signal. In the frequency domain, it is $J(\omega,x) = P(\omega)\delta(x-x^0)$. Applying (2.8), we can get the incident field in the frequency domain which is

$$\begin{aligned} E^{in}(\omega,x) &= -\int G(\omega,x-y)P\omega\delta(y-x^0)dy \\ &= -P(\omega)\frac{e^{ik|x-x^0|}}{4\pi|x-x^0|} \end{aligned} \tag{2.23}$$

Substituting (2.23) to (2.22) we obtain the frequency and time domain expression for the scattered field.

$$E_B^{sc}(\omega,x^0) = p(\omega)\omega^2 \int \frac{e^{2ik|x^0-z|}}{(4\pi)^2|x^0-z|^2} V(z)dz \tag{2.24}$$

$$\mathscr{E}_B^{sc}(t,x^0) = \iint \frac{e^{-i\omega(t-2|x^0-z|/c)}}{2\pi(4\pi|x^0-z|)^2} k^2 P(\omega)V(z)d\omega dz \tag{2.25}$$

Now we apply matched filter to the scattered field to find the output of correlation receiver which is

$$\begin{aligned}\eta(t,x^0) &\approx \int p^*(t'-t)\mathscr{E}_B^{sc}(t,x^0)dt' \\ &= \iint \frac{1}{2\pi}\int e^{i(\omega'-\omega)t'}dt'\frac{e^{-i\omega(t-2|x^0-z|/c)}}{(4\pi|x^0-z|)^2}P(\omega)P^*(\omega')V(z)d\omega' d\omega dz \\ &= \iint \frac{e^{-i\omega(t-2|x^0-z|/c)}}{(4\pi|x^0-z|)^2}k^2|P(\omega)|^2V(z)d\omega dz \end{aligned} \tag{2.26}$$

This equation described the data that is collected by the receiver antenna which we see that it is still a little bit complicated.We are going to simplify it later. We do not look for a Doppler shift since high-range-resolution pulses are considered.We see that the effect of matched filtering is simply to replace $P(\omega)$ by $2\pi|P(\omega)|^2$.

Once more in most cases, the distance between the target and antenna is far larger than the size of an antenna, here we apply far-field to the above equations.[7] When we have $|x| \gg |y|$

$$\begin{aligned}|x-y| &= \sqrt{(x-y)\cdot(x-y)} = \sqrt{|x|^2-2x\cdot y+|y|^2} \\ &= |x|\sqrt{1-\frac{2\hat{x}\cdot y}{|x|}+\frac{|y|^2}{|x|^2}} = |x|\left(1-\frac{\hat{x}\cdot y}{|x|}+O\left(\frac{|y|^2}{|x|^2}\right)\right) \\ &= |x|-\hat{x}\cdot y+O\left(\frac{|y|^2}{|x|}\right)\end{aligned} \tag{2.27}$$

where we used the Taylor expansion$\sqrt{1+a} = 1+a/2+O(x^2)$ and written $\hat{x} = x/|x|$.Note that this far-field expansion involves an implicit choice of an origin of coordinates. Similarly for $|x-y|^{-1}$ we have

$$\frac{1}{|x-y|} = \frac{1}{|x|}\left(1+O\left(\frac{|y|}{|x|}\right)\right) \tag{2.28}$$

Now we apply (2.27),(2.28) with Taylor expansion $e^a = 1+O(a)$ and $(1+a)^{-1} = 1+O(a)$ to the Green's function (2.8) to obtain

$$G(x-y) = \frac{e^{ik|x-y|}}{4\pi|x-y|} = \frac{e^{ik|x|}}{4\pi|x|}e^{-ik\hat{x}\cdot y}\left(1+O\left(\frac{|y|}{|x|}\right)\right)\left(1+O\left(\frac{k|y|^2}{|x|}\right)\right) \tag{2.29}$$

We see that if $|y| \ll |x|$ and $k|y|^2 \ll |x|$, the remainder is very small and could be ignored. Apply (2.29) to (2.26) we have

$$\eta_B(t) \approx \frac{1}{(4\pi)^2|x^0|^2}\int e^{-i\omega(t-2|X^0|/C+2\hat{x^0}\cdot z/c)}k^2|p(\omega)|^2V(z)d\omega dz \tag{2.30}$$

Now apply inverse Fourier transform to (2.30), we have our radar data in frequency domain.

$$D_B(\omega) \approx \frac{e^{2ik|x^0|}}{(4\pi)^2|x^0|^2} k^2 |p(\omega)|^2 \int e^{-2ik\hat{x^0}\cdot z} V(z) dz \tag{2.31}$$

Note that the data D_B is actually collected in three dimensions, according to different imaging situations we will need to project the three dimensional data into two dimensions. After that we need use a interpolation method to translate the polarized data into rectangular data $\tilde{D}_B$. Fig. 2.1 shows the idea of such interpolation. After Fourier transform $\tilde{D}_B$ back to time domain, we got a proper image.

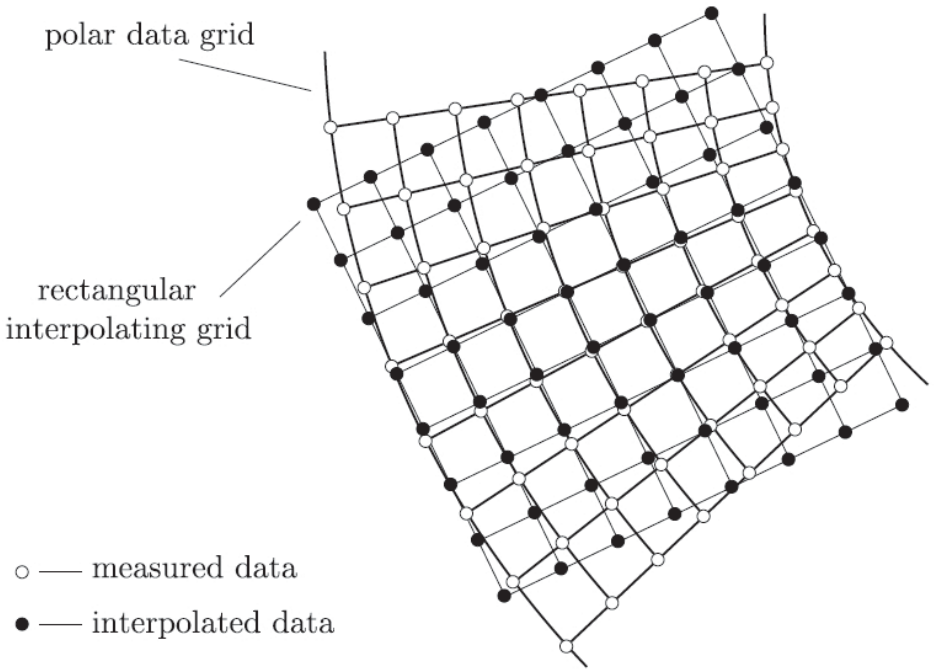

Figure 2.1: The Process of Interpolating from a Polar Grid to a Rectangular Grid

2.2 MIMO Basics

Unlike a normal radar system who usually has only one transmitter and one receiver, a MIMO radar system has multiple transmitting and receiving units. Each transmitting unit could have a completely different waveform to the other transmitting units. This waveform diversity

enables superior capabilities compared with a standard phased array radar system [12, 13] who also has multiple transmitting and receiving units but each unit transmits the same waveform with different a phase or amplitude parameter. Figure 2.2 shows the difference between a MIMO Radar

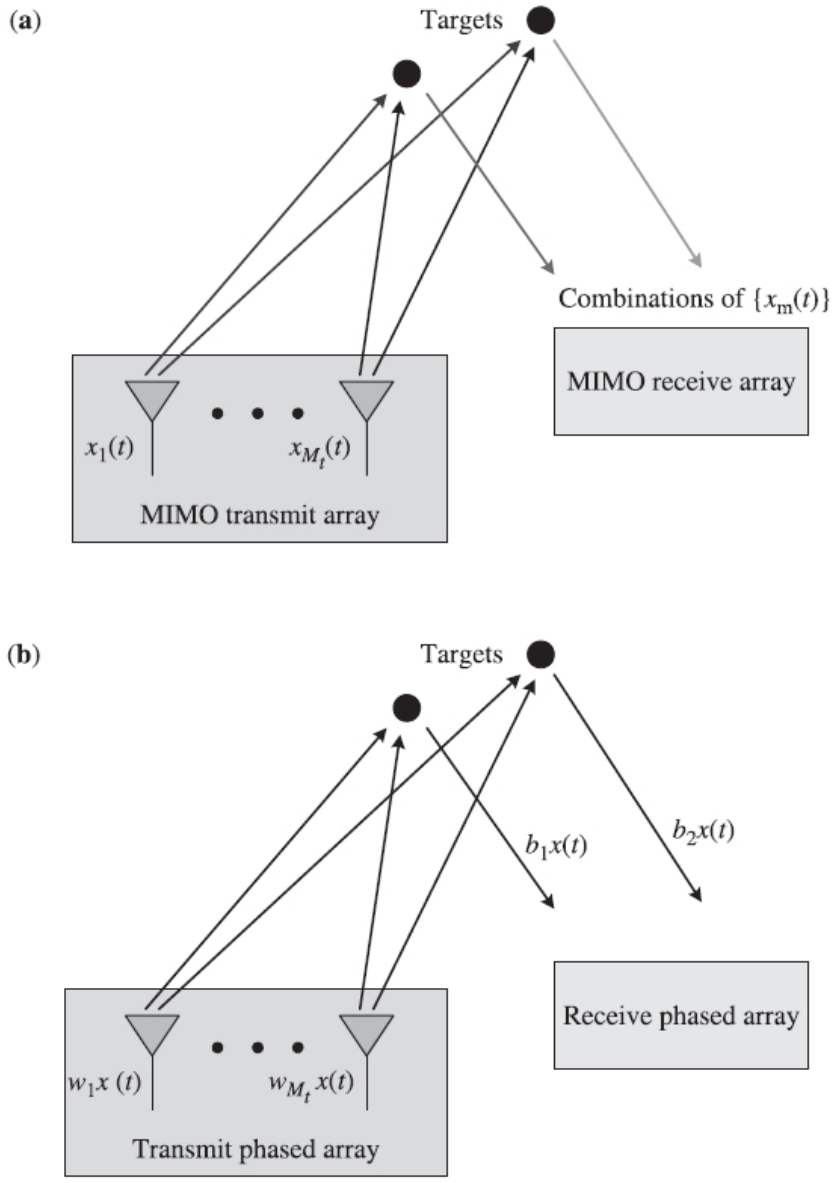

Figure 2.2: MIMO Radar (a) versus Phased-Array Radar(b)

and a Phased-Array Radar.

Consider a MIMO radar system who has M_t transmitting antennas and M_r receiving antennas. Let $X_m(n)$ denote the discrete-time baseband signal transmitted by mth transmit antenna at nth time

sample. Let θ denote the location parameters in a polarized coordinate system, namely its azimuth angle and range. Then with the assumption that the transmitted signals are narrowband and that the propagation is in free space, we have the baseband signal expression at the target location.[14]

$$\sum_{m=1}^{M_t} e^{-j2\pi f_0 \tau_m(\theta)} X_m(n) = \mathbf{a}^*(\theta)\mathbf{x}(n), \qquad n = 1, \cdots, N \tag{2.32}$$

Here f_0 is the carrier frequency of the radar, $\tau_m(\theta)$ the time needed for signal transmitted via the mth transmitting antenna to reach the target, $(\cdot)^*$ is the conjugate transpose, N denotes the number of samples of each transmitted pulse.

$$\mathbf{x}(n) = [x_1(n)x_2(n)\cdots x_{M_t}(n)]^T \tag{2.33}$$

$$\mathbf{a}(\theta) = [e^{-j2\pi f_0 \tau_1(\theta)} e^{-j2\pi f_0 \tau_2(\theta)} \cdots e^{-j2\pi f_0 \tau_{M_t}(\theta)}]^T \tag{2.34}$$

where $(\cdot)^t$ denotes the transpose. If we have the transmit array of the radar calibrated, $\mathbf{a}(\theta)$ is a known function of θ.

Let $y_m(n)$ denote the signal received by the mth receive antenna and

$$\mathbf{y}(n) = [y_1(n)y_2(n)\cdots y_{M_r}(n)]^T \tag{2.35}$$

$$\mathbf{b}(\theta) = [e^{-j2\pi f_0 \tilde{\tau}_1(\theta)} e^{-j2\pi f_0 \tilde{\tau}_2(\theta)} \cdots e^{-j2\pi f_0 \tilde{\tau}_{M_r}(\theta)}]^T \tag{2.36}$$

where $\tilde{\tau}_m(\theta)$ is the time needed for signal scattered by the target at position θ to reach the mth receiving antenna. For simplification we assume that the target is point-like and we will have the received data vector as[14]

$$\mathbf{y}(n) = \sum_{k=1}^{K} \beta_k \mathbf{b}^c(\theta_k)\mathbf{a}^*(\theta_k)\mathbf{x}(n) + \varepsilon(n) \qquad n = 1, \cdots, N \tag{2.37}$$

where K is the number of targets that reflects the signals back to the receiving antenna, β_k stands for the complex amplitude that is proportional to the radar cross sections of the kth target, θ_k is the location parameter of the kth target, $\varepsilon(n)$ is the noise term and $(\cdot)^c$ denotes the complex conjugate.

CHAPTER III

COMPRESSIVE SENSING

The traditional method of reconstructing signals from measured data follows the well-known Nyquist-Shannon sampling theorem [23], which states that the sampling rate must be at least twice the highest frequency of the original signal. Similarly, the fundamental theorem of linear algebra suggests that the number of collected samples of a discrete finite-dimensional signal should be at least as large as its length (its dimension) in order to collect enough information to ensure the full reconstruction of the original signal. This principal is used in most of our current technology such as analog-to-digital conversion, medical imaging and so on.The novel theory of compressive sensing (CS) provides a fundamentally new approach to data acquisition, which overcomes this common wisdom. It states that certain signals are actually sparse in some domain such that it can be recovered by using samples much less than what Nyquist-Shannon theorem requires.

Early development in sparse representation for images and signals are focused on finding the most significant part of the original signal in some space[16, 24, 10]. We actually have the original signal or image already and transform it into a sparse representation. But if we apply this method directly to radar imaging it will cause a problem. We need to collect the data following the Shannon-Nyquist sampling theorem first, then transform the collected data into some function space, compress it with taking the most significant part of the original signal in this specific space, and then recover the image with the compressed signal. What we are doing is actually collecting the full information and then throwing some insignificant part away. Such method works well when we have enough time and space, but it is actually inefficient comparing with taking less samples at the very beginning. Hence given a discrete signal $x \in \mathbb{C}^N$, taking m linear measurements of this

signal is equivalent to applying a matrix $A \in \mathbb{C}^{m\times N}$

$$\mathbf{y} = A\mathbf{x} \tag{3.1}$$

Here A is called the measurement matrix and $\mathbf{y}$ is called the measurement vector. For compressive sensing, we are interested in the case $m \ll N$. Without any other restriction to the problem, this is of course a highly under-determined linear system and hence have infinitely many solutions. But if we have the assumption that the vector $\mathbf{x}$ is a k-sparse, we could transfer this problem to a l_0-minimization problem

$$\min \|z\|_0 \quad \text{subject to} \quad A\mathbf{z} = \mathbf{y} \tag{3.2}$$

Unfortunately, this optimization problem is a NP-hard problem which is computationally unsolvable [15]. Therefore, we need to transform the problem (3.2) into a problem that can be solved . With the assumption that the solution to problem (3.2) is sparse enough,this problem has a unique solution and it is equivalent to the solution of the following l_1-minimization problem[11]

$$\min \|z\|_1 \quad \text{subject to} \quad A\mathbf{z} = \mathbf{y} \tag{3.3}$$

Problem (3.3) is a convex optimization problem which could be solved by some algorithms that already exist, for example, a second-order cone program.

For further analysis on a l_1-minimization we will need the help of following properties[21]. The first one is called the null space property.

Definition 1. *A matrix $A \in \mathbb{C}^{m\times N}$ is said to satisfy the null space property (NSP) of order k with constant $\gamma \in (0,1)$ if*

$$\|\eta_T\|_1 \leq \gamma \|\eta_{t^c}\|_1 \tag{3.4}$$

for all sets $T \subset \{1,2,\cdots,N\}, \#T \leq k$ and for all $\eta \in \ker A$

The following sparse recovery result is based on this definition.

Theorem 1. *Let $A \in \mathbb{C}^{m\times N}$ be a matrix that satisfies the NSP of order k with constant $\gamma \in (0,1)$. Let $x \in \mathbb{C}^N$ and $y = Ax$ and let x^* be a solution of the l_1-minimization* (3.3) *problem. Then*

$$\|x - x^*\|_1 \leq \frac{2(1+\gamma)}{1-\gamma}\sigma_k(x)_1 \tag{3.5}$$

In particular, if x is k-sparse then $x^* = x$.

Here $\sigma_k(x)_1$ is the best k-term approximation of the vector x in l_1 norm, which can be obtained using a non-increasing rearrangement of x. Let $r(x) = (|x_{i_1}|, |x_{i_2}|, \cdots, |x_{i_N}|)$ where i_j denotes a permutation of indexes such that $|x_{i_j}| \leq |x_{i_{j+1}}|$ for $j = 1, \cdots, N-1$, then we have the following expression for $\sigma_k(x)_1$,

$$\sigma_k(x)_1 = \left(\sum_{j=k+1}^{N} |r_j(x)| \right) \tag{3.6}$$

It could be showed that if all k-sparse x can be recovered from $y = Ax$ using l_1-minimization then A has to satisfy the NSP of order k with some constant $\gamma \in (0,1)$ [8]. However, to show a matrix that satisfies NSP directly in real cases are really difficult. Thus we need an easier property which is called the restricted isometry property (RIP) to help us determining either a matrix satisfies NSP or not.

Definition 2. *The restricted isometry constant δ_k of a matrix $A \in \mathbb{C}^{m \times N}$ is the smallest number such that*

$$(1 - \delta_k)\|z\|_2^2 \leq \|Az\|_2^2 \leq (1 - \delta_k)\|z\|_2^2 \tag{3.7}$$

for all z that are k-sparse vectors

Definition 3. *A matrix A is said to satisfy the restricted isometry property of order k with constant δ_k if its restricted isometry constant $\delta_k \in (0,1)$*

It could be showed that if a matrix A satisfies RIP then it satisfies NSP[21].

CHAPTER IV

SIMULATIONS AND RESULTS

In this chapter, we are going to do give a reconstruction algorithm for a ISAR system.

a Random Sampling: For received data of scattered field, we do a random sampling instead of standard sampling requested by Nyquist-Shannon theorem. This means in (3.1), we are choosing a random matrix. In this paper we select partial Fourier matrix which is proved to satisfy restricted isometry property and can be applied to CS reconstruction[6, 17, 20]. This is a matrix of selecting m rows out of a total N rows uniformly with all entries in the selected row

$$F_{j,k} = \frac{1}{\sqrt{N}} e^{2\pi jk/N} \tag{4.1}$$

b Recover the Signal: For sampled data, we use a l_1-minimization method to find the most sparse representation z of the original signal.

c Image Reconstruction: Apply Fourier transform to recovered data to form a image.

Here is the simulation parameters

The main parameters for the below simulations are listed in Table 4.1. To compare with the time-domain CS method, the most common chirp signal is chosen as the transmitted signal. The frequency of chirp signal ranges from 3.0GHz to 3.4GHz.

4.1 Results And Discussion

The image Fig 4.14.2 are two pseudo-targets that is used for simulation. The first one is a ring and the second is a pseudo-aircraft in the form of a combination of scatterers. Figure 4.3

Table 4.1: Main simulation parameters

parameter	Value
speed of EM wave	3.0×10^8 m/s
SFR Starting frequency	3 GHZ
Frequency bandwidth	384 MHZ
Pulse duration	3.3073e-07 s
Pulse repetition frequency	20 KHZ
Initial azimuth angle	0
Angular velocity	0.15 rad/s
Initial distance	1300 m
Look angle	30°
Transmitting Array Size	4
Receiving Array Size	4
Sample rate	0.45×3.4GHZ

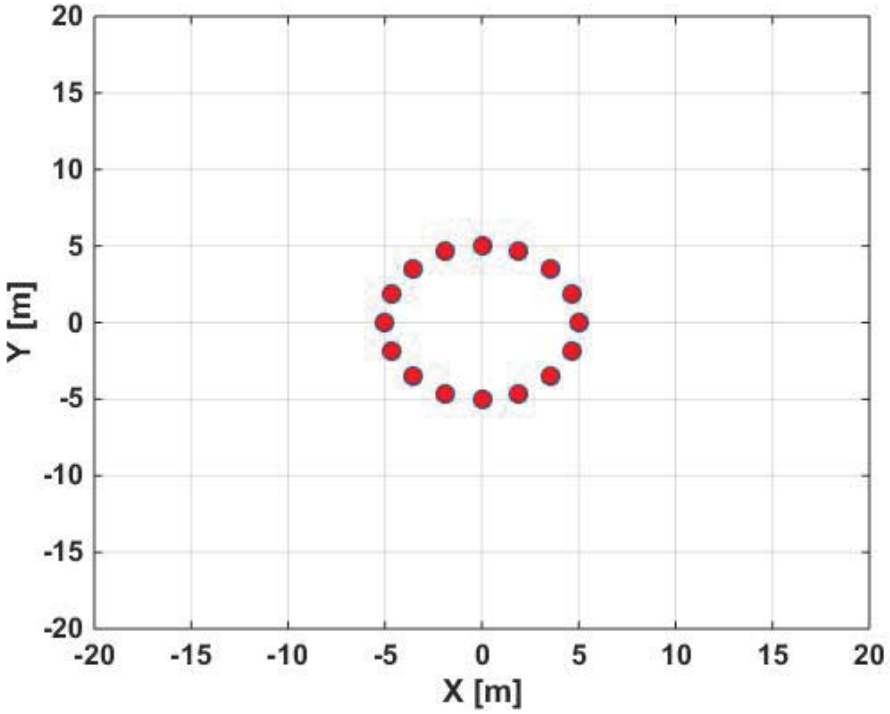

Figure 4.1: Target: A Ring

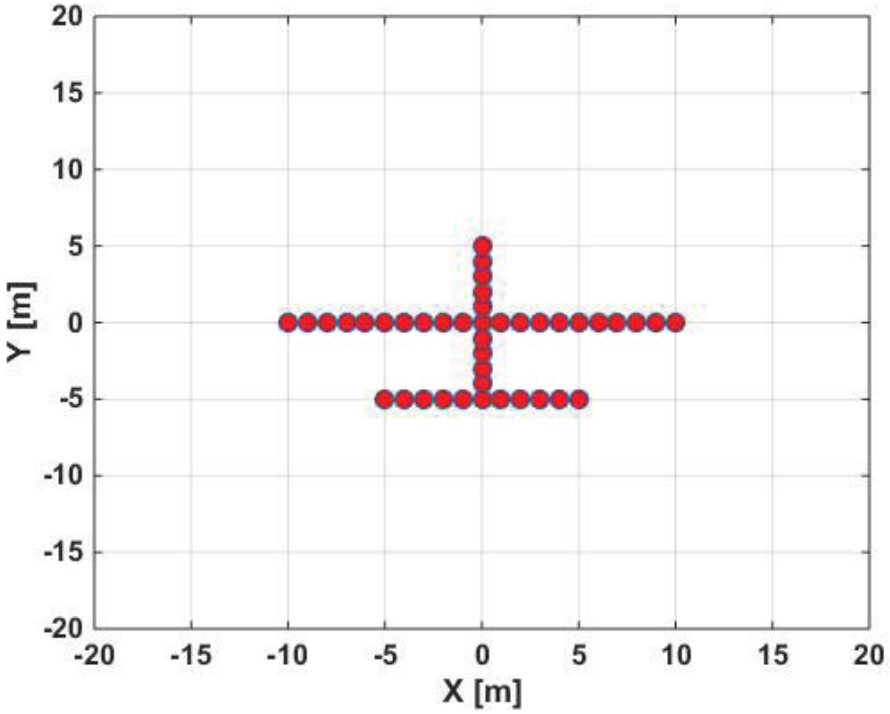

Figure 4.2: Target: A Pseudo-Aircraft

4.4 shows the ISAR Image of the targets under the parameters provided in table 4.1. This image is formed before rotation compensation, so we could see that there are still some parts does not match strictly, but basically it shows what the original object is. Figure 4.5 4.6 shows the image with rotation compensation and we see that it matched the original image exactly.

Now we apply sparse representation to the collected data. Figure 4.7 4.8 are the images generated by sparse representation. We see that there is estimation error added to the original, and clearly we lose some contrast. But considering our sampling rate is only 45% of the highest frequency which is only 22.5% of what is requested by Nyquist-Shannon theorem, this is already a acceptable result. Now we try to apply rotation compensation to both images to improve the quality of the image. The result is given by Figure 4.9 4.10. We see that basically nothing can be distinguished with in the image. Rotation compensation is failed.

4.2 Conclusion And Future Work

In this paper, we used Maxwell equation to derive a far field model of ISAR system. After that, we applied MIMO model and Compressive sensing technology to the original ISAR model and analyzed the the CS problem. This generates the sparse representation of an MIMO ISAR system. In simulation we used a random sample method instead of the original uniform sample and samples at only 22.5% of the original sample rate and get a good result. We still see that with low sampling rate, the image loses SNR and contrast, which leads to a failure on rotation compensation, so the future work of this paper will be increase the quality of the sparse image.

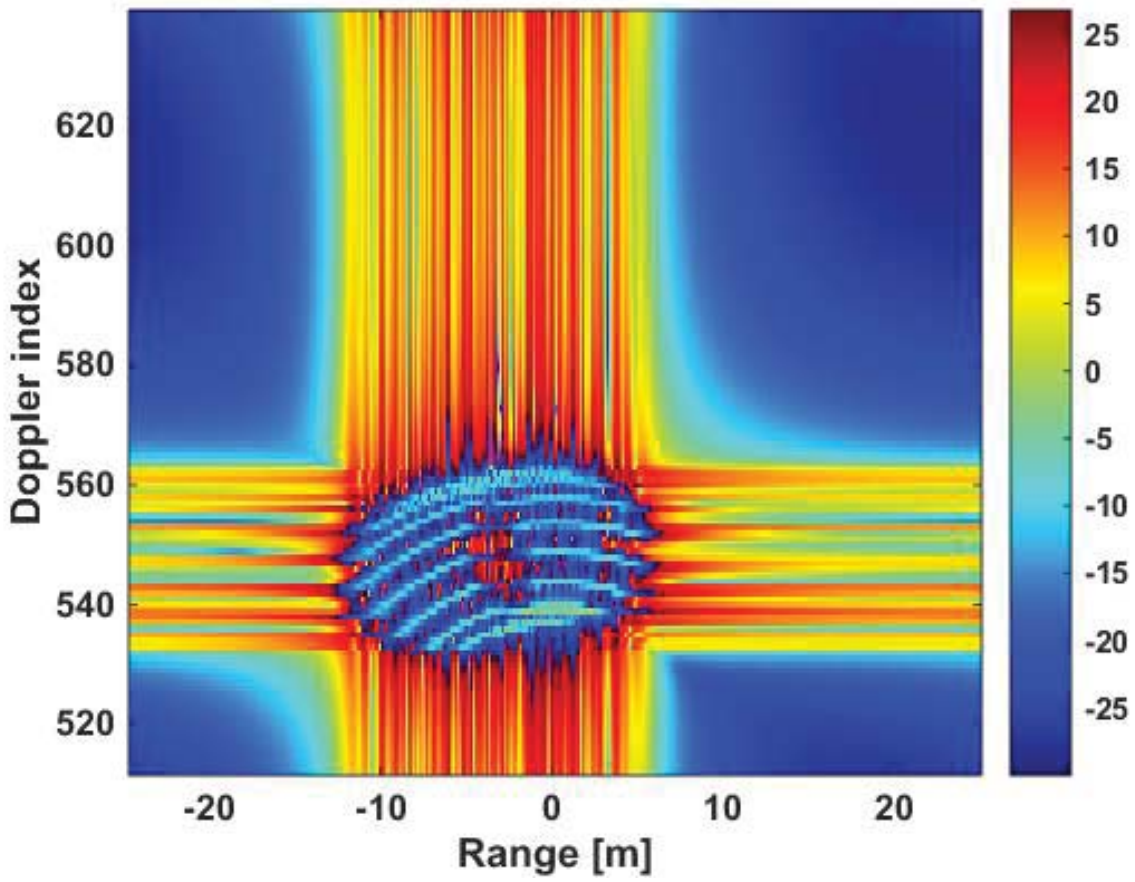

Figure 4.3: ISAR Image of the Ring

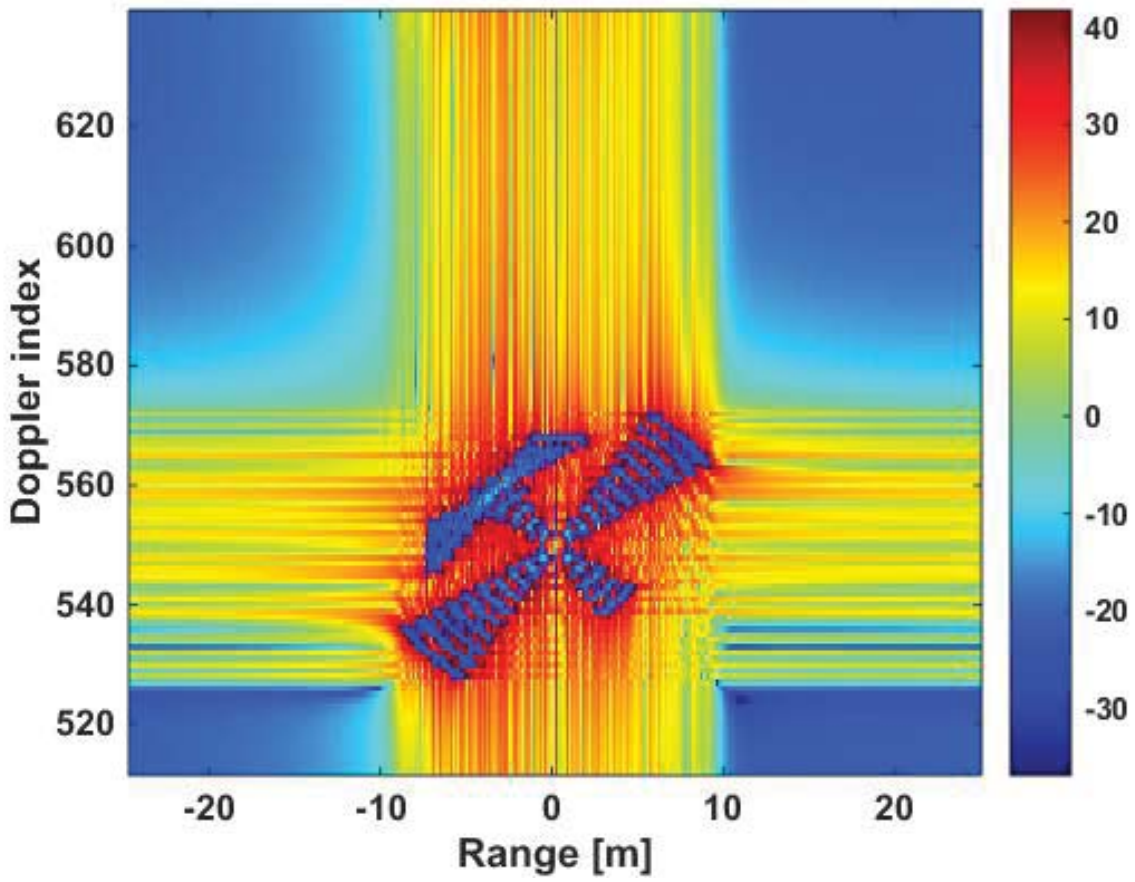

Figure 4.4: ISAR Image of the Pseudo-Aircraft

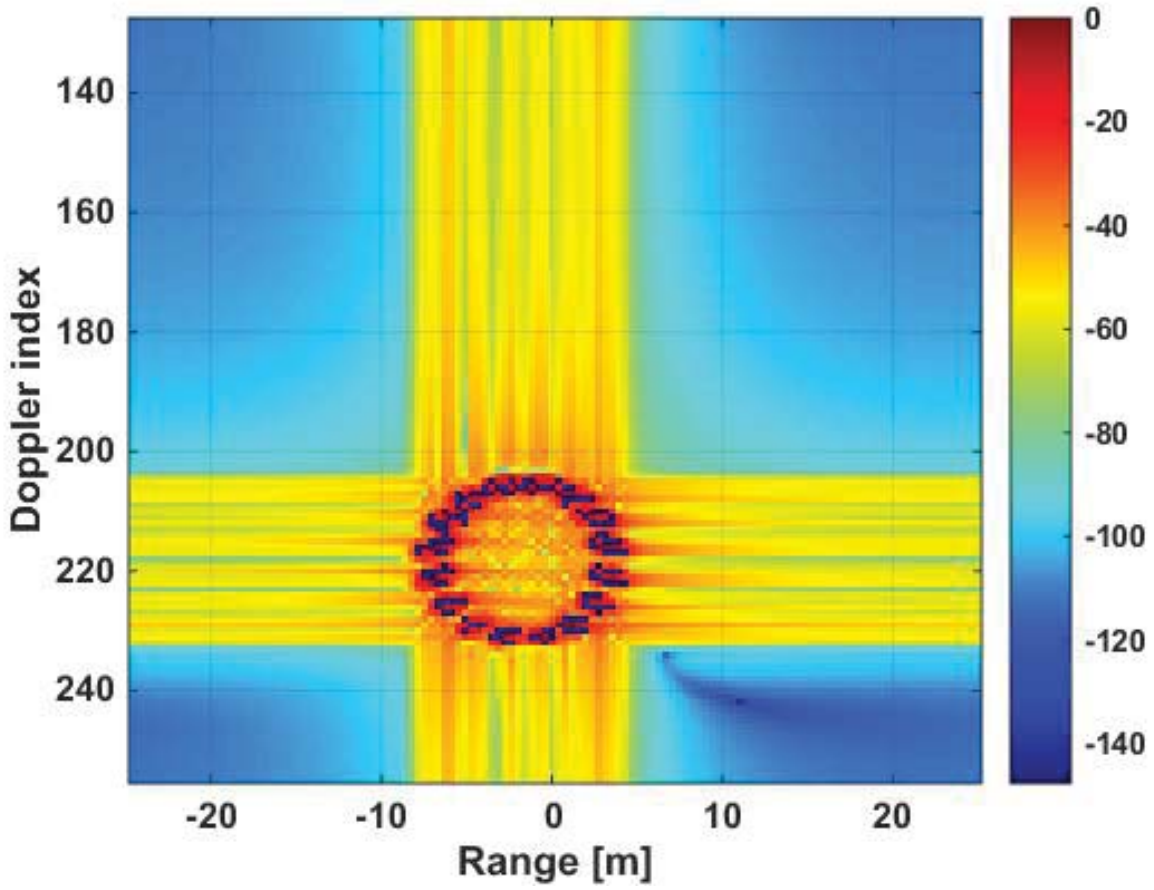

Figure 4.5: ISAR Image with Rotation Compensation of the Ring

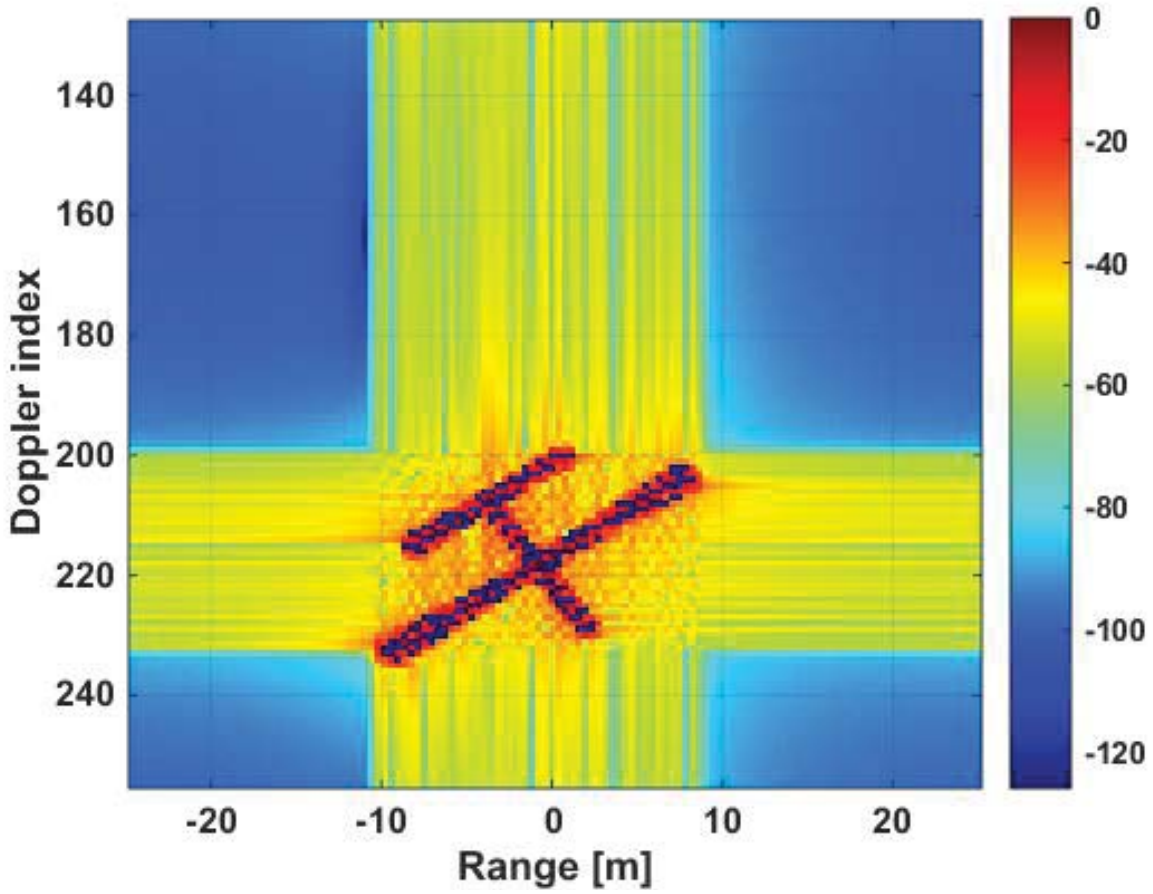

Figure 4.6: ISAR Image with Rotation Compensation of the Pseudo-Aircraft

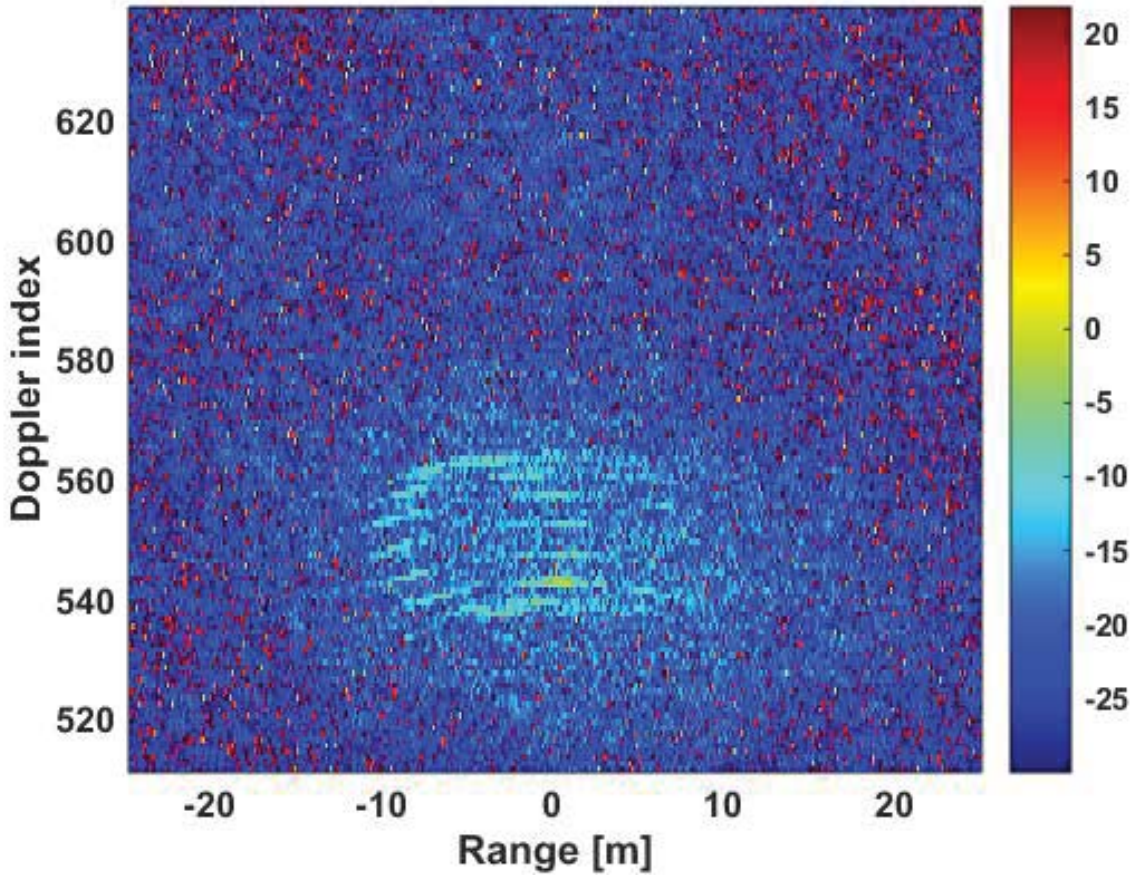

Figure 4.7: ISAR Image with Sparse Representation of the Ring

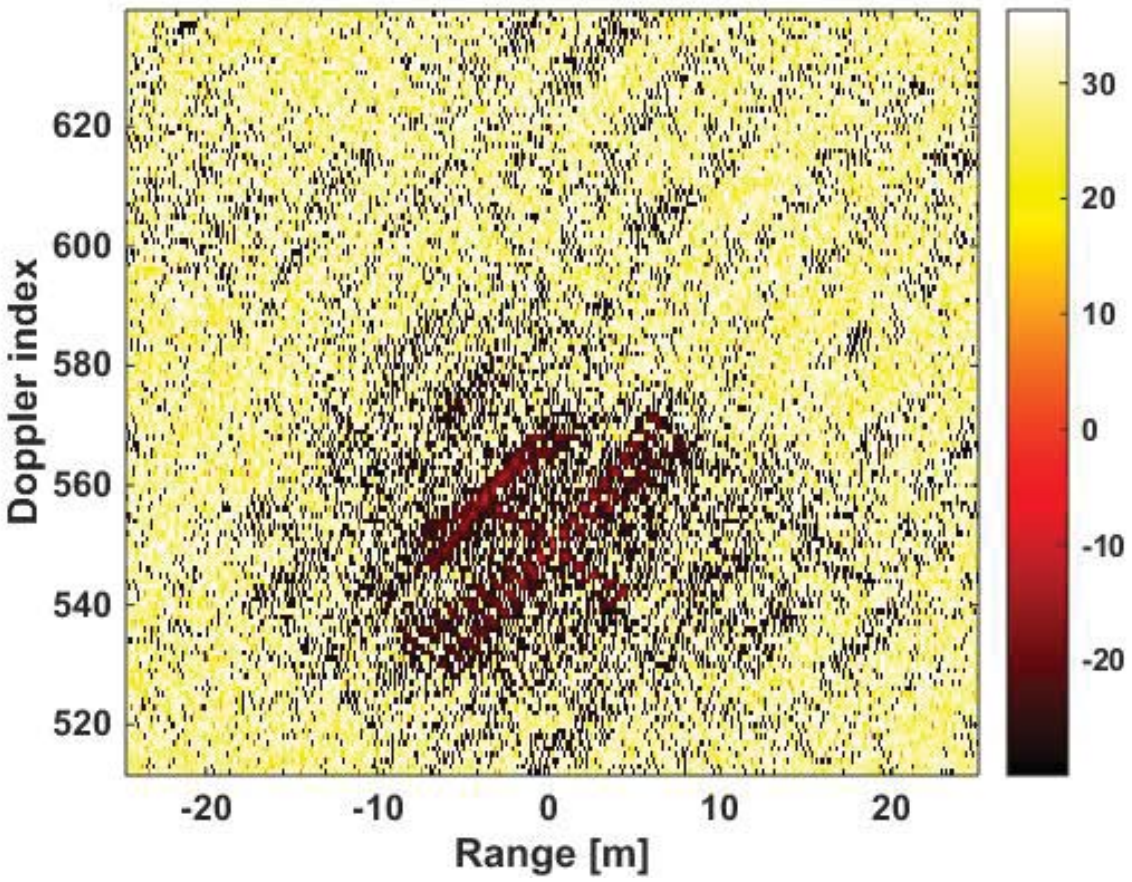

Figure 4.8: ISAR Image with Sparse Representation of the Pseudo-Aircraft

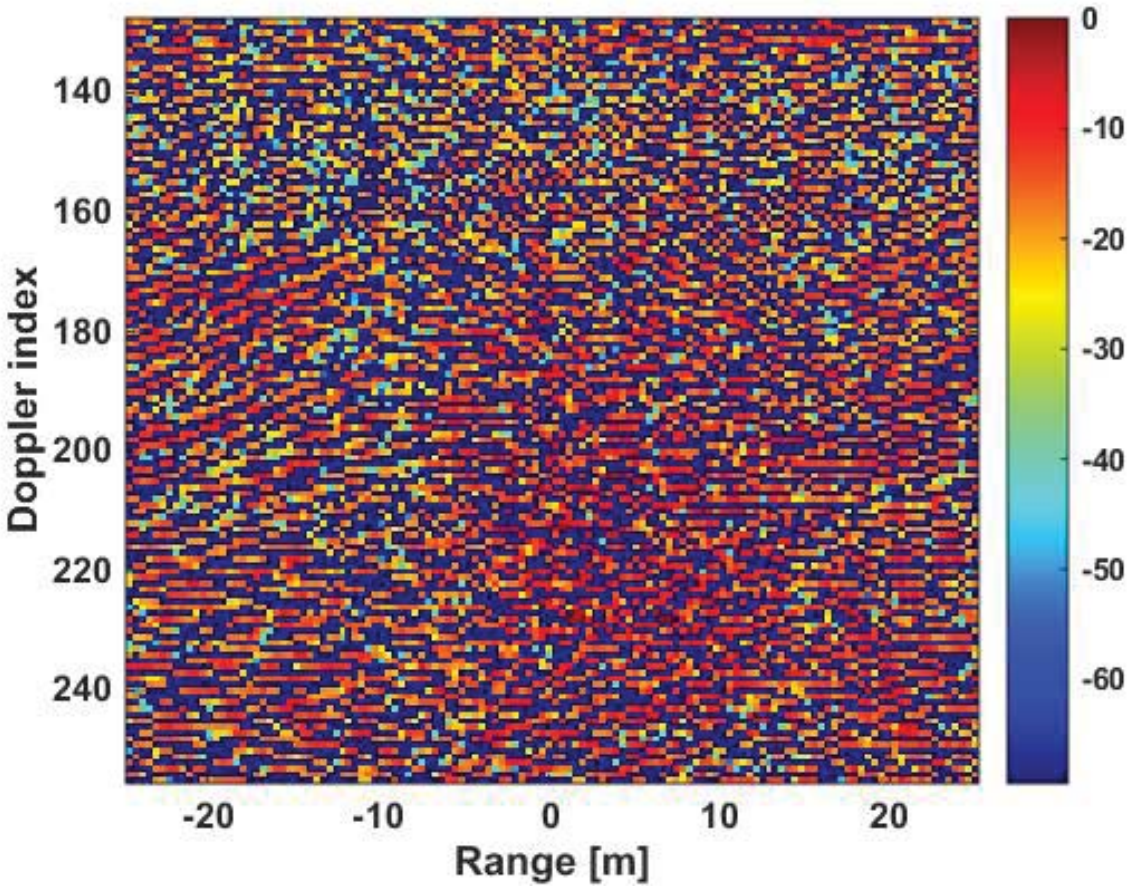

Figure 4.9: ISAR Image with Sparse Representation and Rotation Compensation of the Ring

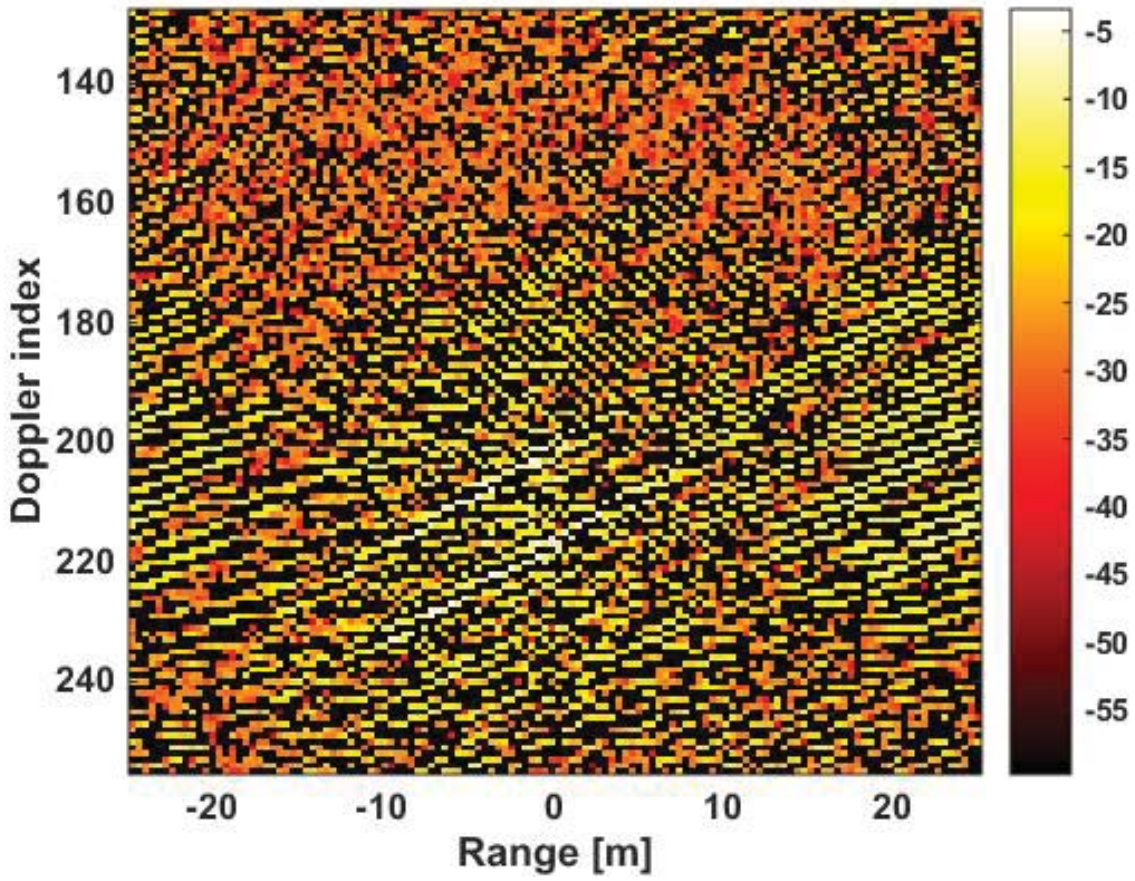

Figure 4.10: ISAR Image with Sparse Representation and Rotation Compensation of the Pseudo-Aircraft

REFERENCES

[1] I. Bekkerman and J. Tabrikian. Mimo radar theory and experimental results. *Signals, Systems and Computers, 2004. Conference Record of the 38th Asilomar Conference on*, pages 300 – 304 Vol.1, 2004.

[2] I. Bekkerman and J. Tabrikian. Target detection and localization using mimo radars and sonars. *IEEE Transactions on Signal Processing*, 54(10):3873 – 3883, 2006.

[3] E.J. Bond, Li Xu, S. C. Hagness, and B. D. Van Veen. Microwave imaging via space-time beamforming for early detection of breast cancer. *IEEE Transactions on Antennas and Propagation*, 59(8):1690 – 1705, 2006.

[4] Emmanuel J. Candès, Justin Romberg, and T. Tao. Robust uncertainty principles: exact signal reconstruction from highly incomplete frequency information. *IEEE Transactions on Information Theory*, 52(2):489–509, 2006.

[5] Emmanuel J. Candès, Justin Romberg, and T. Tao. stable signal recovery from incomplete and inaccurate measurements. *Communications on Pure and Applied Mathematics*, 59(8):1207–1223, 2006.

[6] Emmanuel J. Candès and T. Tao. Near-optimal signal recovery from random projections: Universal encoding strategies. *IEEE Transactions on Information Theory*, 52(12):5406–5425, 2006.

[7] M. Cheney and B. Borden. *Fundamentals of radar imaging*. CBMS-NSF regional conference series in applied mathematics. Society for Industrial and Applied Mathematics (SIAM, 3600 Market Street, Floor 6, Philadelphia, PA 19104), 2009.

[8] A Cohen, W Dahmen, and R DeVore. Compressed sensing and best k-term approximation,(2006). *Preprint*.

[9] J. C. Curlander and R. N. McDonough. *Synthetic Aperture Radar Systems and Signal Processing*. Wiley, 1991.

[10] Ronald A DeVore, Björn Jawerth, and Bradley J Lucier. Image compression through wavelet transform coding. *Information Theory, IEEE Transactions on*, 38(2):719–746, 1992.

[11] David L Donoho. For most large underdetermined systems of linear equations the minimal 1-norm solution is also the sparsest solution. *Communications on pure and applied mathematics*, 59(6):797–829, 2006.

[12] E. Fishler, A. Haimovich, R. Blum, D. Chizhik, L. Cimini, and R. Valenzuela. Mimo radar: an idea whose time has come. In *Radar Conference, 2004. Proceedings of the IEEE*, pages 71–78. IEEE, 2004.

[13] E. Fishler, A. Haimovich, R. Blum, D. Chizhik, L. Cimini, and R. Valenzuela. Spatial diversity in radars-models and detection performance. *IEEE Transactions on Signal Processing*, 54(3):823–838, 2006.

[14] J. Li and P. Stoica. *MIMO Radar Signal Processing*. Wiley, 2008.

[15] S. G. Mallat and Zhifeng Zhang. Matching pursuits with time-frequency dictionaries. *IEEE Transactions on Signal Processing*, 41(12):3397 – 3415, 1993.

[16] William B Pennebaker and Joan L Mitchell. *JPEG: Still image data compression standard*. Springer Science & Business Media, 1992.

[17] Holger Rauhut. Compressive sensing and structured random matrices. *Theoretical foundations and numerical methods for sparse recovery*, 9:1–92, 2010.

[18] M. Reed and B. Simon. *Methods of Modern Mathematical Physics Vol. 1 Functional Analysis*. Academic Press, 1972.

[19] R.C. DiPietro R.P. Perry and R.L. Fante. Sar imaging of moving targets. *IEEE Transactions on Aerospace and Electronic Systems*, 35:188 – 200, 1999.

[20] Mark Rudelson and Roman Vershynin. On sparse reconstruction from fourier and gaussian measurements. *Communications on Pure and Applied Mathematics*, 61(8):1025–1045, 2008.

[21] Otmar Scherzer, editor. *Handbook of Mathematical Methods in Imaging*. Springer, 2010.

[22] F. Treves. *Basic Linear Partial Differential Equations*. Wiley-Interscience publication. Academic Press, 1975.

[23] Michael Unser. Sampling − 50 years after shannon. In *Proceedings of the IEEE*, pages 569 – 587. IEEE, 2000.

[24] Zixiang Xiong, Kannan Ramchandran, and Michael T Orchard. Space-frequency quantization for wavelet image coding. *Image Processing, IEEE Transactions on*, 6(5):677–693, 1997.

[25] YANG YANG and RICK S. BLUM. Mimo radar waveform design based on mutual information and minimum mean-square error estimation. *IEEE Transactions on Aerospace and Electronic Systems*, 43(1):330 – 343, 2007.

[26] Yutao Zhu, Yi Su, and Wenxian Yu. An isar imaging method based on mimo technique. *Geoscience and Remote Sensing, IEEE Transactions on*, 48(8):3290–3299, 2010.

BIOGRAPHICAL SKETCH

Mengqi Hu was born in Xiangtan, Hunan China on June 29 1992. In 2014, he graduated with a B.S. in Mathematics from the Chang'an University in Xi'an, Shaanxi China. After that, he continued his study in mathematics for a master's degree in University of Texas-Pan American, which is now University of Texas Rio Grande Valley. From 2014-2016, he worked on the "Sparse representation for the ISAR image reconstruction". Mengqi has papers published in the Proceedings of the 2015 and 2016 SPIE Defense, Security, and Sensing Conferences. He is awarded Master of Science in Mathematics in August 2016. He can be contacted at qmhu123123@gmail.com.